International Journal of Engineering Innovation & Research
Volume 6, Issue 2, ISSN: 2277 – 5668

Power Components Measurement Using S-ADALINE

Soumyajit Goswami* **Arghya Sarkar** **S. Sengupta**
*email id: soumyajit_goswami@yahoo.com email id: sarkararghya@yahoo.co.in email id: samarsgp@rediffmail.com
*Corresponding author

Date of publication (dd/mm/yyyy): 02/05/2017

***Abstract* — This paper presents the design and implementation of the two stage self-synchronized adaptive linear neural (S-ADALINE) network based novel approach for the measurement of electrical power components according to IEEE Standard 1459-2010. In the first stage, the current and voltage signals are processed to extract the harmonic information, whereas in the second stage, the power components are calculated using these results. The simulation results show that the proposed algorithm provides better performance than the conventional ADALINE and Newton type algorithm (NTA). A simple laboratory setup implemented by MATLAB and dedicated hardware is built to verify the performance of the proposed algorithm in real time applications. The framework of laboratory prototype has been given out and the necessary modification in proposed algorithm for on-line implementation has been discussed.**

***Keywords* — Adaptive Linear Neuron, IEEE Standard 1459-2010, Harmonics, Levenberg Gradient Decent Method, Power Measurements.**

I. INTRODUCTION

Power components (active power, reactive power, apparent power etc.) play very vital role in power system equipment development, compensation device design and tariff calculation. The task of power components' measurement under sinusoidal environments is straight forward and traditional, which becomes challenging and interesting at the presence of harmonics. Lot of efforts have been involved to define power components under harmonic pollution [1]–[2] of which the IEEE Standard 1459–2010 [2] provides latest and comprehensive definitions for the power components by encompassing the well-known sinusoidalconcepts to non-sinusoidal environments. At the same time, advanced digital signal processing algorithms are utilized to measure the power components according to these definitions. The fast Fourier transform (FFT) based algorithm [3], the discrete wavelet transforms (DWT) based approach [4], time domain techniques [5], adaptive resonator based method [6] and decoupled module techniques [7] etc. are example of such efforts. For real-time use, however, there are trade-offs between accuracy and speed for most of the above-mentioned approaches.

In recent years, adaptive algorithms, like the adaptive linear neuron (ADALINE) structure [8] and Newton Type Algorithm (NTA) [9] have attracted much consideration and have been used extensively by means of harmonic estimator due to their simple structure and non-stationary signal tracking ability. However, the conventional ADALINE structure suffers from the following drawbacks:

- It works well at fixed frequency system but utterly fails at off-nominal frequency conditions [10].
- The convergence speed is very slow [11], even though, the steepest descent method based modified Widrow–Hoff weight updating rule provides guaranteed convergence.

On the other hand, the NTA is a faster process but converges only when the initial guess of unknown parameters are near the actual values. In [9], FFT has been utilized to obtain the initial values of the unknown parameters, and thus, significantly increases computational load. Moreover, it fails to converge during abrupt changes of amplitude, phase or frequency.

In [12], a modified ADALINE structure called Self-synchronize ADALINE (S-ADALINE) network, has been developed by the authors which depends on the Levenberg gradient descent (LGD) structure based parameter updating rule and is proficient of handling both nominal and off-nominal frequency conditions.The LGD can be considered as a combination of the steepest descent and the Gauss-Newton method. When the present solution is far away from the exact one, it performs like steepest descent method and offers slow, but guaranteed convergence. On the other hand, when the current solution becomes close to the correct solution, it turns out to Gauss-Newton method and converges rapidly.

This paper presents a potential application of this promising approach in the field of power components instrumentation. In the first stage of the algorithm, the S-ADALINE is utilized for signal frequency and harmonic components estimation. In the second stage, the power components are being calculated according to the IEEE Standard 1459–2010. The obtained simulation outcomes confirm the advantages of the proposed approach over conventional ADALINE based approach and NTA. The experimental results also provided to verify the feasibility of the proposed algorithm for real-time applications.

II. HARMONIC DETECTION WITH S-ADALINE

The S-ADALINE adopted LGD based updating techniques for Fourier-coefficients as well as system frequency identification and has been established as an efficient harmonic detection method due to its simple structure and characteristic of supervised learning mechanism. Brief description of the S-ADALINE based harmonic tracking procedure has been presented below [12].

If, the discrete time input signal y[n] with the fundamental angular frequency comprises a finite number of significant harmonics with maximum order M, then at any sample instant n, it can be represented as

$$\begin{aligned} y[n] &= \sum_{k=1}^{M} Y_k \sin(k\omega_r n + \alpha_k) \\ &= \sum_{k=1}^{M} Y_k \sin(k\omega_r n)\cos\alpha_k + \sum_{k=1}^{M} Y_k \cos(k\omega_r n)\sin\alpha_k \\ &= \sum_{k=1}^{M} G_k \sin(k\omega_r n) + \sum_{k=1}^{M} H_k \cos(k\omega_r n) \end{aligned} \quad (1)$$

where Y_k and α_k are the amplitudes and phase angles of kth harmonic, respectively, $G_k = Y_k \cos\alpha_k$ and $H_k = Y_k \sin\alpha_k$.

By reordering of (1) in matrix form:

$$y[n] = (W[n])^{Tr} x[n] \quad (2)$$

where $W[n] = [G_1 \quad H_1 \quad G_2 \quad H_2 \cdots\cdots G_M \quad H_M]^{Tr}$ (3)

and

$$x[n] = [\sin\omega_r n \;\; \cos\omega_r n \;\; \sin 2\omega_r n \;\; \cos 2\omega_r n \cdots\cdots \sin M\omega_r n \;\; \cos M\omega_r n]^{Tr} \quad (4)$$

Tr indicates transpose of a vector quantity.

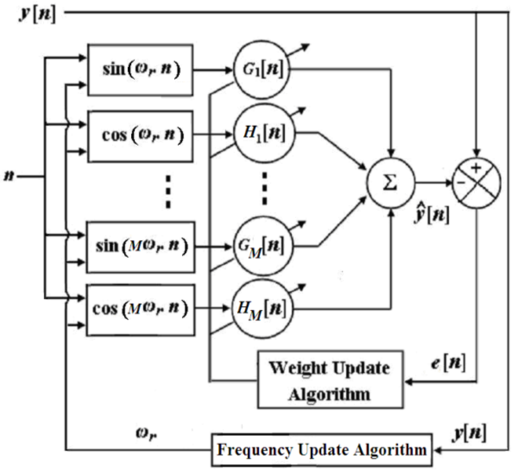

Figure 1: Architecture of the S-ADALINE

The S-ADALINE network can be applied to track the weighting vector W[n] and ω_r adaptively. The overall architecture of the S-ADALINE network for harmonic detection has been presented in Figure 1. The S-ADALINE based harmonic estimation steps [12] are as follows:

Step 1. Initialize adjustable weighting vector WA [0], fundamental angular frequency $\omega_r[0]$, and different constants λ, η_{lmw}, η_{lmf}, and r.

Step 2. Calculate input vector x[n] of (4).

Step 3. Compute the estimation signal

$$y[n] = (W_A[n])^{Tr} x[n].$$

Step 4. Estimate the error signal

$$e[n] = y[n] - (W_A[n])^{Tr} x[n].$$

Step 5. If $e[n] < e_{nom}$, go to Step 8, if not go to ***Step 6.***

Here, e_{nom} is the maximum allowable limit of error signal.

Step6. If $e[n] > e[n-1]$, then $\lambda > \lambda r$, otherwise $\lambda > \lambda / r$ Limit $0.3 \le \lambda \le 100$.

Step7. Update weight vector and fundamental angular frequency as:

$$W_A[n+1] = W_A[n] + \eta_{lmw}\left(x[n](x[n])^{Tr} + \lambda I\right)^{-1} e[n]x[n] \quad (5)$$

$$\omega_r[n+1] = \omega_r[n] + \eta_{lmf}\left((S[n])^2 + \lambda I\right)^{-1} e[n]S[n] \quad (6)$$

Step 8. Go to ***Step 2***.

III. Reformulation Of The Power Components' Definitions

This section delivers single-phase power components' definitions limited to the IEEE Standard 1459–2010 [2] and its reformulation in S-ADALINE domain. The basic assumption is that power system signals have been uniformly sampled at sampling frequency fs, greater than the Nyquist rate, so that aliasing of spectra does not happen.

At steady state situations, the non-sinusoidal instantaneous voltage, v, and current, i, of fundamental angular frequency ω can be presented as

$$\begin{aligned} v &= v_1 + v_K \\ &= \sqrt{2}V_1 \sin(\omega t + \alpha_1) + \sqrt{2}\sum_{k\neq 1}^{M_v} V_k \sin(k\omega t + \alpha_k) \quad (7) \\ &= \sum_{k=1}^{M_v} A_k \sin(k\omega t) + \sum_{k=1}^{M_v} B_k \cos(k\omega t) \end{aligned}$$

$$\begin{aligned} i &= i_1 + i_K \\ &= \sqrt{2}I_1 \sin(\omega t + \beta_1) + \sqrt{2}\sum_{k\neq 1}^{M_i} I_k \sin(k\omega t + \beta_k) \quad (8) \\ &= \sum_{k=1}^{M_i} C_k \sin(k\omega t) + \sum_{k=1}^{Mi} D_k \cos(k\omega t) \end{aligned}$$

where $A_k = \sqrt{2}V_k \cos\alpha_k$ (9)

$B_k = \sqrt{2}V_k \sin\alpha_k$ (10)

$C_k = \sqrt{2}I_k \cos\beta_k$ (11)

$D_k = \sqrt{2}I_k \sin\beta_k$ (12)

α_1, β_1 correspond to the fundamental voltage and current phase angles respectively, while α_k and β_k represent the harmonic voltage and current phase angle respectively, at kth harmonic. v_1, i_1 represent the power system frequency components, and v_H, i_H represent the harmonic components.

A. RMS Calculation

The RMS values of the non-sinusoidal voltage signals with period *T* is

$$V = \sqrt{\frac{1}{hT}\int_{\tau}^{\tau+hT} v^2 dt} = \sqrt{\sum_{k=1}^{M_v} V_k^2} \quad (13)$$

where *h* is a positive integer number.

Using (9) and (10), it can be shown that

$$V=\sqrt{\frac{1}{2}\sum_{k=1}^{M_v}(A_k^2+B_k^2)} \tag{14}$$

Similarly, the expressions of rms value of distorted current signal is

$$I=\sqrt{\frac{1}{hT}\int_{\tau}^{\tau+hT} i^2 dt}=\sqrt{\sum_{k=1}^{M_i} I_k^2} =\sqrt{\frac{1}{2}\sum_{k=1}^{M_i}(C_k^2+D_k^2)} \tag{15}$$

B. Total Harmonic Distortion

The total harmonic distortion of the voltage is given by

$$THD_v=\frac{V_K}{V_1} =\frac{\sqrt{\sum_{k\neq 1}^{M_v}(A_k^2+B_k^2)}}{\sqrt{\left(A_1^2+B_1^2\right)}} \tag{16}$$

The total harmonic distortion of the current is represented as

$$THD_i=\frac{I_K}{I_1} =\frac{\sqrt{\sum_{k\neq 1}^{M_i}(C_k^2+D_k^2)}}{\sqrt{\left(C_1^2+D_1^2\right)}} \tag{17}$$

C. Active Power

The total active power P, fundamental active power P_1 and harmonic active power P_H can be derived as

$$P=\frac{1}{hT}\int_{\tau}^{\tau+hT} vi dt=\sum_k V_k I_k\cos\theta_k =\frac{1}{2}\sum_k\left(A_k C_k+B_k D_k\right) \tag{18}$$

$$P_1=\frac{1}{hT}\int_{\tau}^{\tau+hT} v_1 i_1 dt=V_1 I_1\cos\theta_1 =\frac{1}{2}\left(A_1 C_1+B_1 D_1\right) \tag{19}$$

$$P_H=V_0 I_0+\sum_{k\neq 1} V_k I_k\cos\theta_k =\frac{1}{2}\sum_{k\neq 1}\left(A_k C_k+B_k D_k\right) \tag{20}$$

D. Reactive Power

The total reactive power Q_B, fundamental reactive power Q_1 and harmonic reactive power Q_H can be obtained as

$$Q_B=\frac{\omega_k}{hT}\int_{\tau}^{\tau+hT} i_k\left[\int v_k\right]dt=\sum_k V_k I_k\sin\theta_k =\frac{1}{2}\sum_k\left(B_k C_k-A_k D_k\right) \tag{21}$$

$$Q_1=\frac{\omega_1}{hT}\int_{\tau}^{\tau+hT} i_1\left[\int v_1 dt\right]dt=V_1 I_1\sin\theta_1 =\frac{1}{2}\left(B_1 C_1-A_1 D_1\right) \tag{22}$$

$$Q_H=V_0 I_0+\sum_{k\neq 1} V_k I_k\sin\theta_k =\frac{1}{2}\sum_{k\neq 1}\left(B_k C_k-A_k D_k\right) \tag{23}$$

E. Apparent Power

The total apparent power S, fundamental apparent power S_1, harmonic apparent power S_N, current distortion power D_I, voltage distortion power D_V, harmonic apparent power S_H and harmonic distortion power D_H can be demarcated as

$$S=VI =\frac{1}{2}\sqrt{\sum_k\left(A_k^2+B_k^2\right)\sum_k\left(C_k^2+D_k^2\right)} \tag{24}$$

$$S_1=V_1 I_1 =\frac{1}{2}\sqrt{\left(A_1^2+B_1^2\right)\left(C_1^2+D_1^2\right)} \tag{25}$$

$$S_N=\sqrt{S^2-S_1^2} =\frac{1}{2}\sqrt{\sum_k\left(A_k^2+B_k^2\right)\sum_k\left(C_k^2+D_k^2\right)-\left(A_1^2+B_1^2\right)\left(C_1^2+D_1^2\right)} \tag{26}$$

$$D_I=V_1 I_H =\frac{1}{2}\sqrt{\left(A_1^2+B_1^2\right)\sum_{k\neq 1}^{M_i}\left(C_k^2+D_k^2\right)} \tag{27}$$

$$D_V=V_H I_1 =\frac{1}{2}\sqrt{\left(C_1^2+D_1^2\right)\sum_{k\neq 1}^{M_v}\left(A_k^2+B_k^2\right)} \tag{28}$$

$$S_H=V_H I_H =\frac{1}{2}\sqrt{\sum_{k\neq 1}^{M_v}\left(A_k^2+B_k^2\right)\sum_{k\neq 1}^{M_i}\left(C_k^2+D_k^2\right)} \tag{29}$$

$$D_H=\sqrt{S_H^2-P_H^2} =\frac{1}{2}\sqrt{\left(\sum_{k\neq 1}^{Mv}\left(A_k^2+B_k^2\right)\sum_{k\neq 1}^{M_i}\left(C_k^2+D_k^2\right)\right)^2-\left(\sum_{k\neq 1}\left(A_k C_k+B_k D_k\right)\right)^2} \tag{30}$$

F. Power Factor

The fundamental power factor PF_1 and total power factor PF are represented as

$$PF_1=\frac{P_1}{S_1} =\frac{\left(A_1 C_1+B_1 D_1\right)}{\sqrt{\left(A_1^2+B_1^2\right)\left(C_1^2+D_1^2\right)}} \tag{31}$$

$$PF=\frac{P}{S} =\frac{\sum_k\left(A_k C_k+B_k D_k\right)}{\sqrt{\sum_k\left(A_k^2+B_k^2\right)\sum_k\left(C_k^2+D_k^2\right)}} \tag{32}$$

IV. S-ADALINE Based Power Component Measurement Algorithm

The basic block diagram of the power component measurement algorithm has been presented in Figure 2, in which, S-ADALINE Network 1 and S-ADALINE Network 2 are used to process the scaled down voltage signal *v[n]* and current signal *i[n]*, respectively. The sampling instant, n, along with estimated angular frequencies and previous knowledge of harmonic orders generate input vectors xv[n] and xi[n] which are fed to S-ADALINE Network 1 and S-ADALINE Network 2, respectively. S-ADALINE Network 1 tracks A_k, B_k using xv[n] and weight up-gradation rule, whereas S-ADALINE Network 2 tracks C_k, D_k from $x_i[n]$. The power components have been obtained using equations (13) - (32) based upon the information of converged A_k, B_k, C_k and D_k.

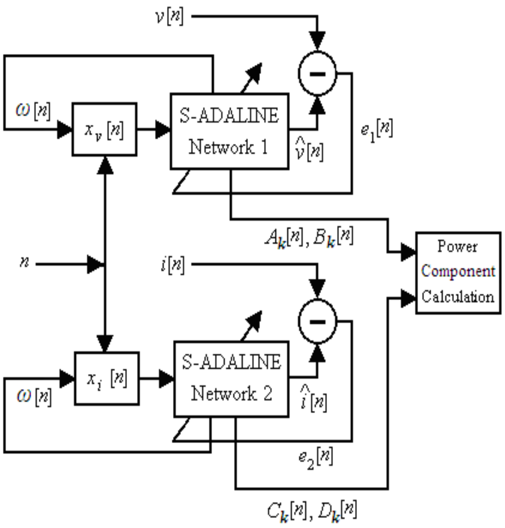

Figure 2: Block diagram of S-ADALINE based power component measurement unit

V. Performance Evaluation Using Simulation

To compare the performance of the proposed algorithm with the conventional ADALINE [14] and Newton-Type Algorithm [9], simulation tests have been performed in MATLAB environment. Primarily, the harmonic tracking capabilities of NTA, proposed S-ADALINE and conventional ADALINE are examined. Then, the accuracy, speed and convergence of the power components estimation algorithms are experimented under steady-state, dynamic and noisy conditions.

The S-ADALINE network has been updated by considering the following initial values: WA = random numbers, λ=100, η_{lmw}=0.4, η_{lmf}=1.6, r= 0.89, ω_r = nominal system angular frequency, weight up-gradation runs until $e[n] \leq 0.0001$. The FFT has been utilized to obtain the initial values of the unknown parameters of the NTA. The sampling rate is taken as 6.4 kHz based on a 50Hz system.

A. Signal Tracking Capability

To test the harmonic tracking capability of this adaptive algorithms at nominal frequency condition (fundamental frequency = 50 Hz), a signal of known harmonic is taken for estimation. The sample waveform is presented as

$$y(t) = \sin\left(\omega_0 t + 29.3^\circ\right) + 0.5\sin\left(3\omega_0 t + 81.0^\circ\right) + 0.1\sin\left(5\omega_0 t - 60.2^\circ\right) \quad (33)$$

The estimation errors in signal tracking for three different algorithms (Conventional ADALINE, NTA and S-ADALINE) have been shown in Figure 3 which shows the proposed S-ADALINE provides faster response than conventional ADALINE and NTA. Theoretically it is true for conventional ADALINE, but surprisingly NTA techniques shows slower convergence than the S-ADALINE. This is basically due to larger value of learning parameter η_{lmf} (in NTA $\eta_{lmw} = \eta_{lmf} = 1$). Moreover, NTA doesn't converge fully and shows small oscillations around steady state value.

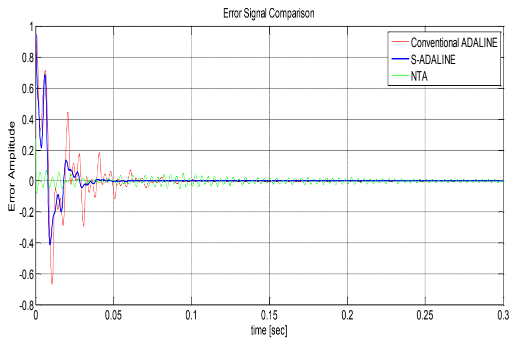

Figure 3: Error Comparison of Conventional ADALINE, NTA and proposed S-ADALINE at Nominal frequency condition (50 Hz)

The estimated amplitude and phase angle of each harmonic component at steady state have been presented in Table 1, which indicates that the accuracies of all the methods except NTA are very high and almost same at nominal frequency.

Table 1: Test Conditions and % Error in Amplitude and Phase Characterization

	Conventional ADALINE		**NTA**		**Proposed S-ADALINE**	
	%Error in Amplitude Est.	%Error in Phase Est.	%Error in Amplitude Est.	%Error in Phase Est.	%Error in Amplitude Est.	%Error in Phase Est.
Fundamental	$1X10^{-4}$	$1X10^{-4}$	$2X10^{-2}$	$3X10^{-2}$	$1X10^{-4}$	$1X10^{-4}$
3rd Harmonic	$2X10^{-4}$	$3X10^{-4}$	$1X10^{-1}$	$2X10^{-1}$	$2X10^{-4}$	$3X10^{-4}$
5th Harmonic	$3X10^{-3}$	$3X10^{-3}$	$2X10^{-1}$	$2X10^{-1}$	$3X10^{-3}$	$3X10^{-3}$

The same waveform is used in off-nominal condition (48 Hz) for the estimation of errors, which have been shown in Figure 4. However, in that case the error of conventional ADALINE is omitted, as it is well-known that conventional ADALINE fails to converge at off-nominal frequency condition.

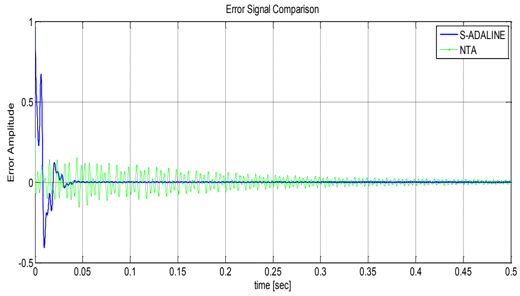

Figure 4: Error Comparison of Conventional ADALINE, NTA and proposed S-ADALINE at Off-nominal frequency condition (48 Hz)

As expected, the proposed S-ADALINE provides better accuracy and faster convergence than the NTA based approach and NTA again exhibits large convergence time.

B. Static Test

The input voltage and current signals used for experiment are given below:

$$v(t)=\sqrt{2}\left[1.0\sin(2\pi ft)+0.03\sin\left(6\pi ft+135^\circ\right)+0.01\sin\left(10\pi ft+150^\circ\right)+0.01\sin\left(14\pi ft+140^\circ\right)\right] \quad (34)$$

$$i(t)=\sqrt{2}\left[1.0\sin\left(2\pi ft+10^\circ\right)+0.3\sin\left(6\pi ft+150^\circ\right)+0.2\sin\left(10\pi ft+155^\circ\right)+0.1\sin\left(14\pi ft-22.5^\circ\right)\right] \quad (35)$$

The estimated power components at nominal frequency (f=50 Hz) are presented in Table 2 which reveals that the proposed method provides much better accuracy (percent errors is of the order of 10-12 %) than NTA (percent errors is of the order of 10-2 %).

Table 2: Power Components Estimation at Nominal Frequency

		IEEE Standard	S-ADALINE based Definitions		NTA based Definitions	
			Measured Values	% error	Measured Values	% error
RMS	V_1	1.0000	1.0000	-0.0005	1.0000	-0.0025
	V_{rms}	1.0005	1.0005	-0.0003	1.0006	-0.0045
	I_1	1.0000	1.0000	-0.0004	1.0001	-0.0057
	I_{rms}	1.0677	1.0676	0.0013	1.0678	-0.0053
Active power	P_1	0.9848	0.9848	-0.0007	0.9849	-0.0108
	P	0.9945	0.9946	-0.0015	0.9946	-0.0117
Reactive power	Q_I	-0.1736	-0.1736	0.0009	-0.1736	0.0047
	Q_B	-0.17516	-0.17518	-0.0037	-0.1752	0.0077
Apparent power	S_1	1.0000	1.0000	-0.0017	1.0001	-0.0098
	S	1.0683	1.0683	-0.0005	1.0684	-0.0089
	S_N	0.3758	0.3759	-0.0102	0.3759	-0.0104

Active power, reactive power and apparent power components at nominal frequency (f=50 Hz) are calculated for the input voltage and current signals (34) and (35). Error to calculate power components for NTA and S-ADALINE are presented in Figure 5. From those power components, Power Factor is also calculated and the error in Power Factor is presented in Table 3 which reveals that the proposed S-ADALINE offers better accuracy than conventional ADALINE and Newton-Type Algorithm

Table 3: Test Conditions and % Error in Power Factor Characterization

	Conventional ADALINE	NTA	Proposed S-ADALINE
% Error in Power Factor	0.366639910113 800	0.7483676175 75003	0.02501849418 9220

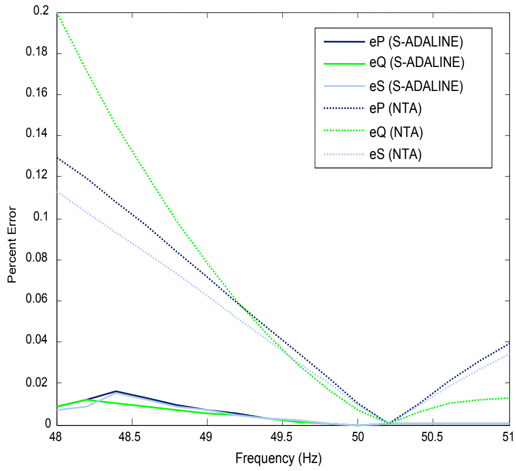

Figure 5: Absolute %errors in power components estimation under off-nominal frequency

C. Dynamic Test

Additional investigations have been taken place to test the performance of the considering algorithms at dynamic condition. In the period from t = 0 to 0.15s, the used test signal is given by (36).

$$y(t)=\sin\left(\omega_0 t+29.3^\circ\right)+0.5\sin\left(3\omega_0 t+81.0^\circ\right) \quad (36)$$

At t = 0.15s, the input signal is rapidly altered to (37). At the same time, the fundamental frequency is also changed from 50 Hz (nominal) to 48 Hz (off-nominal).

$$y(t)=1.4\sin\left(\omega_0 t+50^\circ\right)+0.1\sin\left(3\omega_0 t-60.2^\circ\right) \quad (37)$$

The frequency estimation of the proposed S-ADALINE provides high accuracy and fast convergence compared to the NTA as depicted in Figure 6.

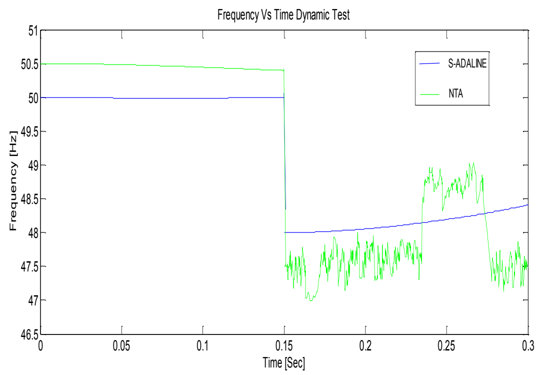

Figure 6: Estimated Frequency Comparison of NTA and proposed S-ADALINE

D. Noise Test

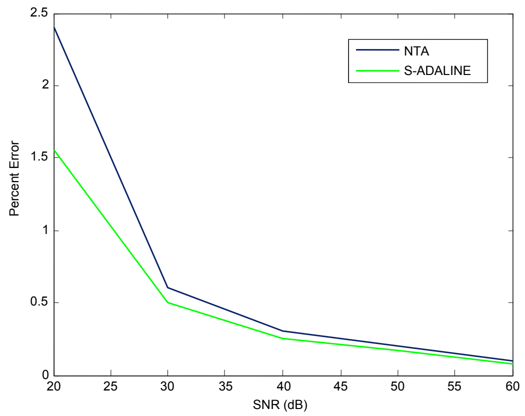

Figure 7: Absolute maximum steady-state errors in active power estimation in terms of SNR

The same input signals (34) and (35) with the superimposed zero-mean white noise has been utilized as input test signals. A range from a highly noisy signal (SNR=20 dB) to a low noisy signal (SNR=60 dB) is covered and, in each case, the steady-state error is measured using the proposed algorithm; and compared with the NTA based technique. As shown in Figure 7, error drops from SNR=20 dB to SNR=60 dB rapidly and S-ADALINE delivers better immunity to noise than NTA.

VI. PC-Based Instrument Development

A. Experimental Setup

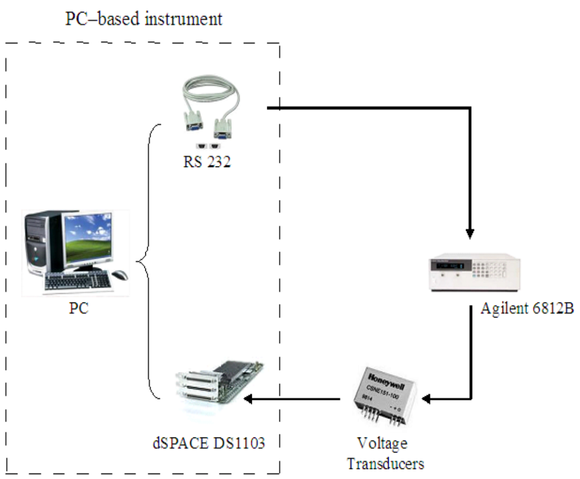

Figure 8: Laboratory test setup for the amplitude tracking

To establish the viability of the proposed algorithm in a real-time environment, it has been experimented physically with the laboratory setup. The developed prototype has been shown in Figure 8, in which the programmable ac power source/power analyzer (PS/PA) Agilent 6812B (750 VA, 300 V, 6.5 A, rms. voltage (35 - 100 Hz) accuracy: $0.03\% + 100\text{mV}$) [16] has been utilized to generate required waveforms. RS 232 bus connects computer (Dual Core Intel Pentium D 3.4 GHz CPU) and PS/PA for signal control.

The experimental system uses a Hall-effect voltage sensor (LEM LV25-P with a 40-µs response time and 0.8% accuracy) for the accommodation of voltage signal from PS/PA to the floating-point controller-board dSPACE DS1103 DSP (four A/D channels—12-b resolution, four A/D channels—14-b resolution, eight A/D channels—12-b resolution, six incremental encoder channels, and a complete subsystem for digital I/O). The proposed strategy is implemented on the DSP system using the SIMULINK (MATLAB toolbox) software package. The sampling time is set to 200 µs. The A/D conversion was performed by means of a 14-b analog-to-digital converter (ADC). Single computer has been utilized to control both the wave form generation and measuring procedure.

B. Third-Order Iterative Matrix Inversion Method

The computational complexities and response time of the proposed S-ADALINE are primarily influenced by inversion of the Hessian matrix($H[n] = x[n]\left(x[n]\right)^{Tr} + \lambda I$). To reduce the computational burden in real time implementation, the third-Order Iterative method, as presented in [15] has been utilized here.

If, $A = [a_{i,j}]_{NXN}$ is an iterative matrix with real or complex elements and the initial guess V_0 satisfies $\| I - AV_0 \| < 1$, then with third convergence order,

$$A^{-1} \; [illegible] \; {}_n(3I - AV_n(3I - AV_n)) \qquad (38)$$

Where, I is the Identity matrix and iteration number $n = 0, 1, 2, \ldots.$

This is an effective tool for constructing iterative methods of high order of convergence to calculate matrix inversion mathematically for all types of matrices (especially for ill-conditioned).

C. Experimental Results

Agilent 6812B is programmed through PC to create test signals, as presented in (36) & (37). Since, the primary influence to the uncertainty of the instrument is due to the transducers, in order to evaluate the uncertainties related only the measurement algorithm, at the first stage of the experimentation no transducer has been utilized. In the next stage, the effect of the transducers has been considered. The maximum absolute measurement errors with and without transducer have also been presented in Table 4.

Table 4: Accuracy Characterization

Power Components	Maximum Absolute Measurement %Errors (without transducer)	Maximum Absolute Measurement %Errors (with transducer)
Active Power	$4X10^{-3}$	$8X10^{-2}$
Reactive Power	$1X10^{-3}$	$3X10^{-2}$
Apparent Power	$3X10^{-3}$	$7X10^{-2}$

Experimental results show that the peak absolute measurement errors during "without transducer" experimentation are very low and in accordance with those obtained by simulations. The accuracies are mainly influenced by the bit limitation effect of the software/hardware implementation unit. As expected, the uncertainties introduced by the transducers are relatively predominant. However, the PC-based instrumental setup with voltage transducer does not still exceedClass-I limits (± 1% of the nominal values), as defined in IEC Standard 61000-4-7 [17].

VII. Conclusion

A modified algorithm for the digital metering of power components according to IEEE Standard 1459-2010 is showcased with extensive experiments. It is based on the application of the S-ADALINE, which is an improved approach for real time implementation of the ADALINE. The S-ADALINE is able to synchronize itself with system frequency and can estimate the spectrum at the exact harmonic order of interest. The obtained results confirm an advantage in improved accuracy, better immunity to noise, and faster convergence than the conventional ADALINE & NTA approaches. A simple laboratory implementation, based on MATLAB and the dedicated hardware, confirms the feasibility of the proposed algorithm for real-timeapplications.

References

[1] Arseneau, R., Baghzouz, Y., Belanger, J., Bowes, K., "Practical definitions for powers in systems with nonsinusoidal waveforms and unbalanced loads: A discussion," *IEEE Trans. Power Delivery* 11 (1996), 79-101.
[2] IEEE Standard 1459-2010, *IEEE standard definitions for the measurement of electric power quantities under sinusoidal, non sinusoidal, balanced or unbalanced conditions*, IEEE Standard, March 2010.
[3] Islam, M., Mohammadpour, H. A., Ghaderi, A., Brice, C. W., & Shin, Y. J., "Time-frequency-based instantaneous power components for transient disturbances according to IEEE standard 1459," *IEEE Transactions on Power Delivery*, *30*.3 (2015), 1288-1297.
[4] Manimala, D., and D. Sundararajan, "Evaluation of IEEE standard 1459-2010 power components using stationary wavelet transform." *Advanced Computing and Communication Systems (ICACCS), 2016 3rd International Conference on*., vol. 1. IEEE (2016), 1 - 6.
[5] Cataliotti, V. Cosentino, S. Nuccio, "A virtual instrument for the measurement of IEEE Std 1459-2000 power quantities," in *Proc Instrumentation and Measurement Technology Conference - IMTC (2005)*, Ottawa, Canada, 1513-1518.
[6] J. J. Tomi´c, M. D. Kušljevi´c, and D. P. Marˇceti´c, "An adaptive resonator-based method for power measurements according to the IEEE trial-use standard 1459–2000," *IEEETrans. Instrum. Meas*., 59 (2010), 250 - 258.
[7] M. D. Kušljevi´c, "A simultaneous estimation of frequency,magnitude, and active and reactive powerby using decoupled modules," *IEEETrans. Instrum. Meas*. 59 (2010), 1866 - 1873.
[8] T. K. Abdel-Galil, E. F. El-Saadany and M.M. A. Salama, "Power qualityevent detection using Adaline," *Electr. Power Syst. Res.* 64 (2003), 137–144.
[9] V. V. Terzija, V. Stanojevi´c, M. Popov, and L. Sluis, "Digital metering of power components according to IEEE Standard 1459-2000 using the Newton-type algorithm," *IEEETrans. Instrum. Meas*. 56 (2007), 2717 - 2724.
[10] Arghya Sarkar, S. Sengupta, "On-line tracking of single phase reactive power in non-sinusoidal conditions using S-ADALINE networks," *Measurement*, 42 (2009), 559 - 569.
[11] G. W. Chang, C. I. Chen, B. C. Huang, and Q. W. Liang, "A comparative study of two weights updating approaches used in ADALINE for harmonics tracking," in *Proceedings of the ICHQP* 2 (2008), 1 – 5.
[12] A. Sarkar, S. Roy Choudhury, and S. Sengupta, "A self-synchronized ADALINE network for on-line trackingof power system harmonics," *Measurement* 44 (2011) 784 - 790.
[13] P. K. Dash, S. K Panda, A. C. Liew, B. Mishra, and R. K. Jena, "A new approach to monitoring electric power quality," *Electric Power Systems Research* 46 (1998), 11 - 20.
[14] P. K. Dash, A. C. Liew and SaifurRahaman, "An Adaptive Linear Combiner for On-line Tracking of Power System Harmonics," *IEEETrans. Power Systems* 11 (1996), 1730 - 1735.
[15] H.-B. Li, T.-Z. Huang, Y. Zhang, V.-P. Liu, T.-V. Gu, "Chebyshev-type methods and preconditioning techniques", *Appl. Math. Comput.* 218 (2011), 260–270.
[16] Agilent Technologies, User's Guide AC Power Solutions Agilent Models 6811B, 6812B, and 6813B, Sep. 2004.
[17] Electromagnetic Compatibility (EMC) – Part 4: Testing and Measurement Techniques – Section 7: General Guide on Harmonics and Interharmonics Measurement and Instrumentation for Power Supply Systems and Equipment Connected Thereto, IEC 61000-4-7, 2002

Authors' Profile

Soumyajit Goswami was born in West Bengal, India on August 27, 1983. He obtained his B.E. (Electrical & Communication Engineering) from Vidyasagar University, Kolkata, India and M.Tech (Computer Science & Engineering) from West Bengal University of Technology, Kolkata, India. His employment experience includes about eleven years in different industries.He is presentlya research fellow with the West Bengal University of Technology and working with IBM India Pvt. Ltd. His special fields of interest include Power Quality, DSP and Soft Computing.

Arghya Sarkar obtained his B. Sc. (Physics Honours), B. Tech., M.Tech and Ph.D. in Electrical Engineering from University of Calcutta, Kolkata, India. He is presently working with MCKV Institute of Engineering, Liluha, Howrah, West Bengal, India. His special fields of interest include Power Quality, DSP and Control System.

Samarjit Sengupta (*MIEEE*) obtained B. Sc. (Physics Honours), B. Tech., M.Tech and Ph.D. in Electrical Engineering from University of Calcutta, Kolkata, India. His employment experience includes about nine years in different industries and about twenty-fiveyears of teaching and research in the Department of Applied Physics, University of Calcutta, Kolkata, West Bengal, India. His special fields of interest include Power Quality and power system stability.